



Cite this: *Nanoscale*, 2015, 7, 20025

Electrical release of dopamine and levodopa mediated by amphiphilic β -cyclodextrins immobilized on polycrystalline gold†

Giulia Foschi,^{‡a} Francesca Leonardi,^{§‡b} Angela Scala,^{¶c} Fabio Biscarini,^a Alessandro Kovtun,^b Andrea Liscio,^b Antonino Mazzaglia^{*c} and Stefano Casalini^{*§a}

Vesicles of cationic amphiphilic β -cyclodextrins have been immobilized on polycrystalline gold by exploiting the chemical affinity between their amino groups and Au atoms. The presence of cyclodextrins has been widely investigated by means of AFM, XPS, kelvin probe and electrochemical measurements. This multi-functional coating confers distinct electrochemical features such as pH-dependent behavior and partial/total blocking properties towards electro-active species. The host–guest properties of β -cyclodextrins have been successfully exploited in order to trap drugs, like dopamine and levodopa. The further release of these drugs was successfully achieved by providing specific electrical stimuli. This proof-of-concept led us to fabricate an electronic device (*i.e.* an organic transistor) capable of dispensing both dopamine and levodopa in aqueous solution.

Received 10th August 2015,
Accepted 28th October 2015

DOI: 10.1039/c5nr05405b

www.rsc.org/nanoscale

Introduction

Over the last decade, the proper combination of materials science and nanotechnology has led to the so-called “nanoarchitectonics”.¹ The proper processing of nano-compounds and eventually their immobilization on a substrate of interest allows one to fabricate new multi-functional interfaces, which can be exploited in different fields such as electrochemical capacitors, super-capacitors, biosensors, drug release systems, bioreactors *etc.*²

Within this context, cyclodextrins (CyDs) can be proficiently exploited. CyDs are trunk-shaped cyclic oligosaccharides composed of 6, 7 or 8 α -D-glucopyranose units, known as α -, β - and

γ -CyDs respectively.³ Among the wide library of CyD-derivatives, amphiphilic CyDs (ACyDs) are promising candidates because they outdo the natural CyD features.⁴ ACyDs are synthesized by grafting a hydrophobic moiety (*viz.* alkylthio chain) and an hydrophilic functionality (*viz.* polyethylene glycol chain, PEG) on the narrow and the wide rim of CyDs.⁵ This backbone enables the formation of bilayer vesicles in aqueous solution, in which the lipophilic chains are hydrophobically entangled yielding the vesicle membrane, whereas the hydrophilic chains are exposed to the outer environment (see Fig. 1a). These vesicles show multi-functional properties since they act as “liposomes” entirely composed of macrocyclic hosting molecules. Nowadays, a wide library of ACyDs is available owing to their versatile synthesis, and they can be classified as a function of their outer charges (*viz.* non-ionic, cationic and anionic ones). For instance, the presence of various terminal groups (*i.e.* $-\text{NH}_2$ group) allows ACyDs to adhere and pass through the cell membrane.^{6,7} Furthermore, they can host and/or entrap a wide library of guests, such as antiviral⁸ and antimitotic drugs,⁹ metal-photosensitizers for photo-activated or photo-independent anticancer therapies,^{10–12} or DNA for gene delivery.¹³ A proper combination of ACyDs and metals enables the achievement of a multi-functional vector for phototherapeutic purposes.^{14,15} As a result, cationic amphiphilic β -CyDs ($\text{A}\beta\text{CyDs}$) endowed with porphyrins can be successfully casted on quartz substrates yielding photo-responsive films¹⁶ or forming bilayer vesicles capable of strongly interacting with gold nanoparticles (AuNPs).¹⁵ The molecular interactions between cationic $\text{A}\beta\text{CyD}$ vesicles and AuNPs have

^aUniversità degli Studi di Modena e Reggio Emilia, Dipartimento di Scienze della Vita, via Campi 183, I-41100 Modena, Italy. E-mail: stefano.casalini@unimore.it

^bCNR-ISOF Istituto per la Sintesi Organica e la Fotoreattività, v. Gobetti n.101, I-40129 Bologna, Italy

^cCNR-ISMN Istituto per lo Studio dei Materiali Nanostrutturati, Dipartimento di Scienze Chimiche, Biologiche, Farmaceutiche ed Ambientali dell'Università di Messina, Viale F. Stagno D'Alcontres 31, I-98166 Messina, Italy.

E-mail: antonino.mazzaglia@ismn.cnr.it

† Electronic supplementary information (ESI) available: Kelvin probe, AFM and electrochemical data are reported. Furthermore, the chemical backbone of both types of cyclodextrins are shown. See DOI: 10.1039/c5nr05405b

‡ Authors who equally contributed.

§ Dr F. Leonardi and Dr S. Casalini are working at the Institut de Ciència de Materials de Barcelona (ICMAB-CSIC), 08193 Bellaterra (Spain).

¶ Present address: Dipartimento di Scienze Chimiche, Biologiche, Farmaceutiche ed Ambientali, Università di Messina, Viale F. Stagno D'Alcontres 31, I-98166 Messina, Italy.

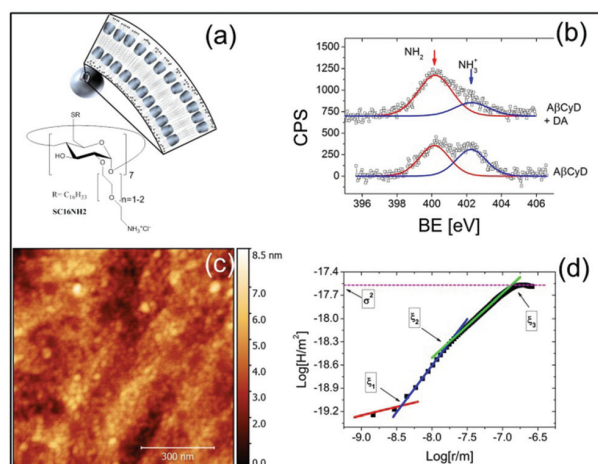


Fig. 1 (a) Chemical backbone of A β CyD and its assembly yielding a cationic vesicle. (b) Comparison of the N 1s spectra for the samples of (up) A β CyD and (down) A β CyD loaded by DA. (c) AFM image (1 μm^2) of Au functionalized by cationic A β CyD vesicles. (d) Log–Log plot of the height–height correlation function. Red, blue, green and pink lines are linear fits.

been widely investigated, pointing the crucial role exerted by the $-\text{NH}_2$ group.¹⁵ The preferential coordination of AuNPs with the amino group, rather than the thioether group, agrees with a poor accessibility of the sulphur atom because of its steric hindrance imposed by the whole structure of the vesicles. These nanoconstructs can entrap polar and/or apolar drugs, thus forming a delivery system with potentially high therapeutic efficacy.

In parallel, organic electronics have witnessed a dramatic boost towards biomedical applications, since organic transistors, such as the electrolyte-gated organic field-effect transistors (EGOFETs), can be successfully operated in an aqueous environment without any additional capping layer.¹⁷ This enabled us to fabricate low-power electronic devices whose operational voltages are lower than 1 V.¹⁸ Their extreme versatility along with easy material processing led to the fabrication of wearable electronics not only on the skin,¹⁹ but also on internal organs (*viz.* heart, brain, spinal cord *etc.*).^{20–23} For instance, a multi-tasking platform was recently designed and applied onto the skin, whose layout brings together mechanical sensors, non-volatile memory and a complex system of drug release.²⁴ Another stretchable platform was successfully implanted into the spinal cord in order to provide both electrical recording/stimuli and a local drug delivery.²⁵

Here, our main objective was the immobilization of cationic A β CyD vesicles onto Au electrodes. Although a wide literature is present on the exploitation of cyclodextrins as electrode modifiers,²⁶ the role of the surface tension of a solid support upon the A β CyD-based vesicles adsorption has been solely studied. In the case of poor chemical affinity between vesicles and substrates, the adsorption of these vesicles can yield monolayer and/or bilayer coatings.²⁷ In this approach, we take advantage of the chemical affinity between the Au and amine groups

in order to develop a multi-functional electrode by means of a one-step process. This multi-functional electrode is capable of releasing electrical neurotransmitters, such as dopamine (DA) and levodopa (L-DOPA). Furthermore, we have integrated our A β CyD-coated electrode in an EGOFET layout, aiming to the development of smart technology for biomedical applications.

Results and discussion

Kelvin probe and X-ray photoemission

The simple immersion of the Au electrode in a solution containing cationic A β CyD vesicles (see Fig. 1a) allowed us to yield a stable coating on this metal (see the Experimental section).

Kelvin Probe (KP) and X-Ray Photoemission Spectroscopy (XPS) measurements have been performed. KP has allowed us to monitor the contact potential difference (CPD) of the electrode at each functionalization step (see Fig. S1 in the ESI†).²⁸ Although this technique provides a qualitative view of the Au surface due to the complexity of the A β CyD coating, clear changes are induced. A more accurate description has been achieved by means of XPS. In fact, the vesicle immobilization is driven by the interaction of nitrogen atoms with the Au surface. For this reason, N 1s spectra have been monitored, showing unambiguously the presence of A β CyD after the Au immersion in the vesicle dispersion. In particular the presence of two nitrogen chemical species have been detected such as ammonium (NH_3^+) and amino (NH_2) groups, set respectively at 402.3 eV and 400.2 eV, in good agreement with the literature^{15,28} (see Fig. 1b). Quantitatively, we observe a change in the relative intensities of the two peaks where the $\text{NH}_2/\text{NH}_3^+$ ratio, which passes from $1.3(\pm 0.2)$ to $2.8(\pm 0.3)$. The doubling of this value strongly indicates the presence of dopamine that possesses an additional amino group (*i.e.* NH_2). This proof is also confirmed by an increase in the signal of nitrogen with respect to the gold one (data not shown).

AFM and electrochemical assessment of A β CyD functionalization

The adsorption of bilayer vesicles is a complex process, which involves not only the transition from free vesicles in solution to immobilized ones onto a solid support, but also other phenomena such as rupture, coalescence and fusion.^{29,30} Although a detailed study of the coating morphology is beyond the scope of this work, we have performed AFM on a flat region of the Au electrode (see Fig. 1c). By using the Height–Height Correlation Function (HHCF), morphological descriptors such as the root mean square roughness (σ_{rms}), the lateral correlation length (ξ) and the roughness exponent (α) have been determined,^{31,32} as shown in Fig. 1d.

Moving from bare (see Fig. S2†) to A β CyD-coated Au (see Fig. 1c and d), we observe a rougher surface together with a lower number of correlation lengths. These can be considered two distinct fingerprints of the A β CyD immobilization (see Table S1†). In particular, the bare Au features σ_{rms} as low as 0.89 (± 0.01) nm with respect to the A β CyDs-coated one, whose σ_{rms} is

equal to $1.64(\pm 0.01)$ nm. Concerning functionalized Au, ξ_1 and ξ_2 are ascribable to the circular species, whose correlation lengths are equal to $3.7(\pm 0.1)$ nm and $18.6(\pm 0.3)$ nm respectively. The size discrepancy is relevant with respect to the radius (*i.e.* 30 nm) of the free vesicles in aqueous dispersion, thus deeper surface analysis is required in order to elucidate the effective reason of this shrinkage.³³ Finally, ξ_3 of A β CyD-coated Au can be safely ascribed to the atomic ordering of Au, because this correlation length is similar to the uncoated one.

These cationic vesicles are adsorbed onto the Au surface due to their amino groups that are situated at the end of the oligoethylene glycol chain in the A β CyDs hydrophilic portion.¹⁵ To support our rationale, we have performed the same experiment by using non-ionic A β CyD vesicles, as a reference experiment. These vesicles feature hydroxyl groups instead of amine ones, and they cannot be immobilized onto Au (see Fig. S3†). Cyclic voltammetry (CV) and electrochemical impedance spectroscopy (EIS) have been performed as described in the Experimental section. The peak to peak distance (ΔE_p), namely the difference of the cathodic and anodic peaks, is a parameter directly connected to the reversibility of the electron transfer (ET) between ferricyanide and Au. ΔE_p higher than 60 mV means lowering of the electron transfer rate with respect to the ideal redox reaction.³⁴ In parallel, EIS set to the redox potential of ferricyanide allowed us to extract the charge transfer resistance (R_{CT}) and capacitance (C) by means of the Randles circuit.³⁵ As shown in Fig. S4 and S5,† this ensemble of the parameters describes quantitatively the unsuccessful immobilization of the non-ionic vesicles compared with the cationic ones.

Further experimental evidence of the immobilization of the cationic vesicles on the Au electrode was gained from the electrochemical study of the redox signal of ferricyanide as a function of pH (*viz.* from 3 to 12). The cationic A β CyD vesicles bear amine groups that are protonated/unprotonated by changing pH, hence the overall positive charges onto Au. As a result, CV (see Fig. 2a) and EIS (see Fig. 2b) measurements were per-

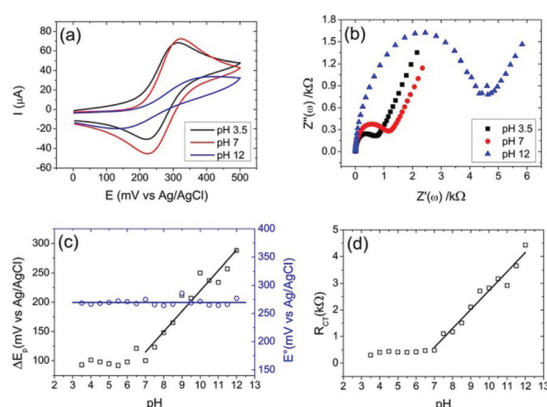


Fig. 2 (a) Cyclic voltammograms and (b) Nyquist plots of the redox signal of $[\text{Fe}(\text{CN})_6]^{3-/4-}$ in acidic (pH 3.5), neutral (pH 7) and alkaline (pH 11) solutions. (c) Peak-to-peak distance (black empty squares) and redox potential (blue empty circles) are plotted as a function of pH. (d) pH-dependence of the charge transfer resistance.

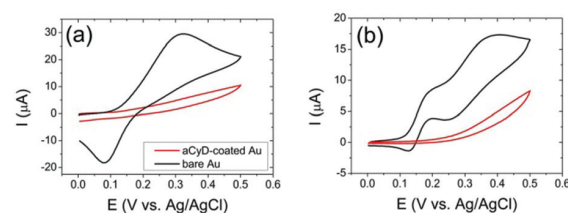


Fig. 3 Overlay of cyclic voltammograms for bare (black line) and A β CyDs coated Au (red line) corresponding to 1 mM of DA (a) and L-DOPA (b) in a phosphate buffered solution (100 mM at pH 7).

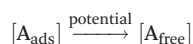
formed as described in the Experimental section. As shown in Fig. 2c, acidic and neutral environments show values centred around 100 mV of ΔE_p featuring a quasi-reversible redox reaction. Beyond neutral conditions, ΔE_p has a linear increase featuring a slope of $35(\pm 3)$ mV per pH because of a slower ET rate than the acidic/neutral state. Furthermore the redox potential of ferricyanide is invariant as a function of pH, in fact its redox reaction does not involve protons. The impedance spectroscopy confirms this trend. Regarding the EIS measurements, the R_{CT} is irrespective of pH variations from 3 to 7, whereas the alkaline range induces a linear increase of the overall impedance with slope equal to $0.71(\pm 0.04)$ kΩ per pH (see Fig. 2d). All these pieces of evidence show how $[\text{Fe}(\text{CN})_6]^{3-/4-}$ interact electrostatically with the cationic vesicles adsorbed onto Au. In particular, acidic and neutral environments keep the amino groups protonated present in the vesicles thus maximizing the electrostatic attraction between them and ferricyanide. Moving towards alkaline buffer, the amino group gets uncharged due to its deprotonation ($\text{p}K_a$ equal to 9),³⁶ and this weakens this type of interaction. For this reason the overall ET slowing down in an alkaline environment is perfectly coherent to the electrostatic view. Within this context, an additional proof of the A β CyD vesicles grafted on the Au electrode is the blocking properties towards positively electroactive species. As a result, DA and L-DOPA are electrochemically active featuring well-known faradaic current ranging from +200 mV and +300 mV (*vs.* Ag/AgCl).³⁷ By comparing the bare and vesicle-coated Au, it is clear how the adsorbed A β CyD vesicles are blocking the redox reactions of these two compounds with respect to the bare electrode as shown in Fig. 3a and b.

In terms of current response, the faradaic current of the bare Au is turned into a purely capacitive after the surface functionalization. This further proof stems from the above-mentioned electrostatic screening of the vesicle-based coating towards positively charged species such as DA and L-DOPA at a neutral pH.³⁸

Electrical release of dopamine and L-DOPA

As mentioned in the introduction, A β CyD vesicles give rise not only to electrostatic interactions tunable by pH, but they also can act as a drug “catcher” by means of host–guest interactions. Since β CyDs have been widely used to host dopamine and its derivatives,^{39–43} we have decided to incubate our func-

tionalized electrodes in DA and L-DOPA solutions (see the Experimental section). These A β CyD-coated and drug-loaded electrodes have been electrically stressed by iterative voltammetric cycles centred at the redox potential of DA/L-DOPA. As shown in Fig. 4, 20 cycles are sufficient to follow the total disappearance of the anodic peak. This means that iterative cycling can induce the detachment of DA and L-DOPA trapped in the cationic vesicles. Since it is known that DA and its derivatives can be partially adsorbed on bare Au,^{44,45} we compared A β CyDs-coated Au (see Fig. 4a, c and e) and the bare one (see Fig. 4b, d and f) after the immersion in DA/L-DOPA solutions. This allowed us to undertake an accurate evaluation of the A β CyD role during the electrical release. Firstly, the A β CyD-coated electrode shows more resolved anodic peaks (see Fig. 4a and c) than the bare ones (see Fig. 4b and d) featuring a more efficient ET. On the contrary, the cathodic peak is completely quenched for A β CyD-coated Au, because the vesicle-based coating screens electrostatically the Au electrode against positive species, as previously described. Furthermore, the kinetics of the release has been characterized by monitoring the anodic peak. The kinetic mechanism has been fitted as a first order reaction (see Fig. 4e and f):



in which $[A_{\text{ads}}]$ is the drug trapped, $[A_{\text{free}}]$ is the species released by the electrical field.

The dataset has been successfully fitted by the following equation:

$$[A_{\text{free}}] = A_{\text{max}} (1 - e^{-\beta n})$$

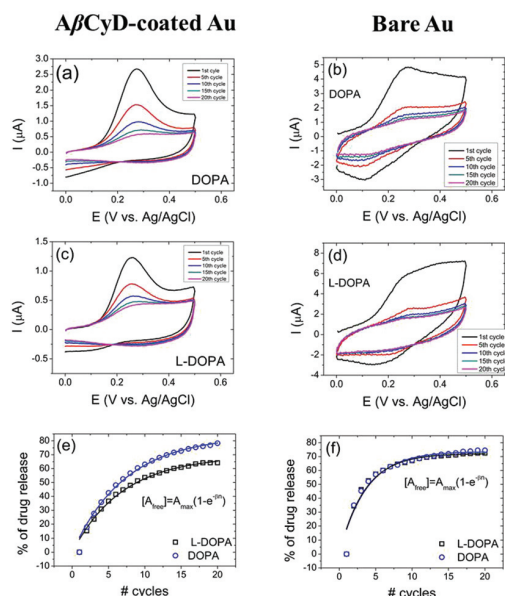


Fig. 4 Electrical release of DA and L-DOPA for A β CyDs-coated Au (a, c, e) and bare one (b, d, f). Fit of the electrical release of both drugs corresponding to functionalized (e) and bare Au (f).

Table 1 A_{max} , β and $n_{1/2}$ have been extracted using the 1st order reaction equation and are listed here

	A_{max} (%)	β (cycle ⁻¹)	$n_{1/2}$ (cycle)
A β CyD coated Au [DA]	84 (± 2)	0.14 (± 0.01)	4.9 (± 0.3)
A β CyD coated Au [L-DOPA]	69 (± 2)	0.14 (± 0.01)	4.9 (± 0.3)
Bare Au [DA]	74 (± 2)	0.27 (± 0.02)	2.6 (± 0.2)
Bare Au [L-DOPA]	72 (± 2)	0.29 (± 0.03)	2.4 (± 0.2)

where A_{max} is the maximum amount of DA/L-DOPA released, β is the kinetic rate and n is the number of voltammetric cycles. As you can see in Table 1, the release mediated by A β CyD vesicles has the same half lifetime ($n_{1/2}$), however the overall amount of released DA is higher than L-DOPA. On the contrary, the $n_{1/2}$ of bare Au is half compared to the functionalized Au, featuring a faster process, whose A_{max} is the same for both drugs. This agrees with an aspecific adsorption of both neurotransmitters onto the bare Au with respect to the host-guest interactions occurring when Au is functionalized by A β CyD vesicles.

Drug dispenser based on electrolyte-gated organic field-effect transistor (EGOFET)

In light of these properties, it has been decided to integrate the A β CyD coated-Au electrode as the gate of an EGOFET. This device can be coupled to aqueous solutions, because it is water-stable and capable of working at low operational voltages (*i.e.* <1 V). Furthermore, these devices are extremely sensitive towards surface modifications by exploiting organic compounds and/or bio-species.^{46–50} In particular, we have monitored the different states of this gate surface: (i) bare, (ii) A β CyDs grafting, (iii) DA/L-DOPA loading and (iv) its release. I - V transfer (see Fig. 5a) and output (see Fig. 5b) characteristics have been consequently acquired. The electrical performances

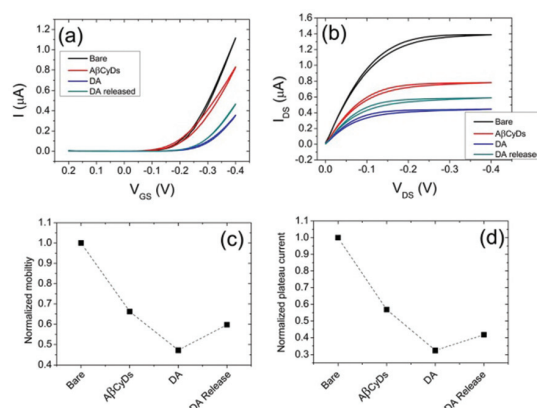


Fig. 5 I - V transfer (a) and (b) output characteristics corresponding to each step of the functionalization protocol. (c) Mobility and (d) the maximum current of the output characteristics are plotted for each functionalization step.

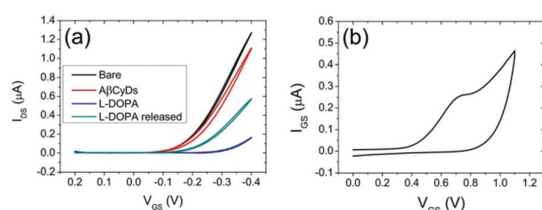


Fig. 6 (a) Overlay of the I - V transfer characteristics for bare Au (black line), A β -CyDs-coated Au (red line), L-DOPA loading (blue line) and L-DOPA release (green line). (b) I - V graph of the leakage current corresponding to the L-DOPA release.

of the reference EGOFET (*i.e.* the uncoated Au electrode) are aligned to the standard behaviour of a water-gate organic transistor, whose working principle is based on the capacitive coupling between the gate electrode (*i.e.* polycrystalline Au) and the organic semiconductor (*i.e.* pentacene). Small hysteresis and leakage current at the nA scale are fingerprints that no electrochemical doping occurs during the whole experiment.^{51,52} The field-effect mobility (see Fig. 5c) and the plateau current (see Fig. 5d) have been extracted from I - V transfer and output characteristics for each surface treatment. These two parameters are consistent, because the subsequent addition of biochemical species on the gate electrode are responsible for a progressive resistive drop at the gate/electrolyte interface.^{49,50} This is also coherent with the CPD trend extracted by the KP measurements, which monitors the effective changes of surface potential due to the presence of different distribution of dipoles onto the metal surface.^{53,54}

Furthermore, it has been successfully verified how the electrochemical release of the drug can be directly managed by an EGOFET (see Fig. 6a and b) with respect to the previous experiment, where the drug release has been achieved by using an electrochemical cell. After the usual characterization of the different functionalization steps (Fig. 6a), the source and drain electrodes have been grounded and short-circuited, and the gate-source current (I_{GS}) sweeping from 0 V to 1.1 V has been monitored (Fig. 6b).

An anodic peak has been observed around 700 mV owing to the drug release. This setup exploits the gate electrode as a working electrode, whereas the organic semiconductor acts as a counter electrode. By comparing EGOFET and a standard electrochemical cell, the presence of an insulating film of pentacene onto the source and drain along with the absence of a reference electrode gives rise to a potential discrepancy in the two systems.

Experimental

Preparation of A β CyD solution and Au functionalization

Both cationic and non-ionic A β CyDs vesicles (see Fig. 1a) of SC₁₆NH₂ or SC₁₆OH were prepared following the protocol published elsewhere.³³ Briefly, SC₁₆NH₂/SC₁₆OH were dissolved in dichloromethane (0.1 mg ml⁻¹) and slowly evaporated under

N₂. This organic film was re-dispersed in aqueous solution (bi-distilled water) by using ultrasonic bath for 5 h at RT. In parallel, polycrystalline Au wires (\varnothing 1 mm) were cleaned as follows: (i) immersion in concentrated H₂SO₄ at 100 °C for 1 h; (ii) 20 cycles of electropolish sweeping the potential from 0 V to 1.5 V in H₂SO₄ (1 M).⁵⁵ These electrodes have been then immersed in aqueous solution containing the cationic vesicles overnight. The final step was a further immersion of the A β CyD-coated Au in an aqueous solution of DA or L-DOPA (1 mM) for 30 min.

Kelvin probe

Kelvin probe measurements were performed under ambient conditions using a 2 mm diameter gold tip amplifier (Ambient Kelvin Probe Package from KP Technology Ltd). The technique provides a voltage resolution of about 5 mV. Calibration and monitoring of the probe were performed using a freshly prepared gold surface. A comprehensive description of the technique can be found in a study by Baikie *et al.*⁵⁶

X-ray photoemission

The XPS spectra were recorded under UHV conditions (5×10^{-10} mbar) with a Phoibos 100 hemispherical energy analyser (Specs) using Mg K α radiation ($h\nu = 1253.6$ eV). The X-ray power was 250 W. The spectra were recorded in the constant analyser energy (CAE) mode with an analyser pass energy of 20 eV. The peaks were fit with symmetric Voigt function processed by CasaXPS v.2.3.16 software. The calibration of the binding energy was performed by using the Au 4f_{7/2} peak (BE = 84.0 eV) from the substrate and the C 1s signal at 285.0 eV from surface contamination.

AFM imaging

AFM Solver Platform SMENA (NT-MDT Moscow, Russia) operated in an intermittent contact mode was used for scanning the surface of polycrystalline Au functionalized by cationic A β CyD vesicles (see Fig. 1c). In particular, AFM has been performed onto golden slides purchased from Arrandee (Germany) and flame annealed as described in their datasheet. This instrument is equipped with a camera for positioning the cantilever on selected areas of the sample. AFM data analysis was carried out with Gwyddion 2.30 software.

Electrochemical measurements

The electrochemical measurements are performed by an usual three-electrode cell connected to a potentiostat/galvanostat μ -Autolab type III (Metrohm Italiana S.r.l., Varese, Italy), using a polycrystalline Au wire, as a working electrode (WE), functionalized with the above-mentioned protocol; a Pt sheet and Ag/AgCl were used as counter (CE) and reference (RE) electrodes respectively. The ferricyanide signal has been monitored by cyclic voltammetry (CV) and electrochemical impedance spectroscopy (EIS). The former has been carried out between 0 V and +500 mV (*vs.* Ag/AgCl) with a scan rate of 100 mV s⁻¹. The latter has been performed fixing the set-point voltage at the redox potential (namely E°) of [Fe(CN)₆]^{3-/4-} with an

amplitude of 10 mV scanning from 10^5 Hz to 10^1 Hz. The Nyquist plots have been fit by using the Randles equivalent circuit, which allows us to extract the charge transfer resistance (R_{CT}) and the capacitance (C) of the material deposited onto the working electrode. The electrolytic solutions with a known pH consisted of phosphate buffer (100 mM) and NaCl (0.1 M). The pH adjustments have been achieved by using small aliquots of NaOH and HCl.

Electrical characterization of electrolyte-gated organic field-effect transistor (EGOFET)

Test-patterns have been purchased from Fondazione Bruno Kessler (Trento, Italy). The substrate is quartz (optical grade) with a roughness lower than 2 nm. The Au leads are 40 nm thick with an adhesive layer of Cr (3–4 nm thick). The W/L ratio is around 2000. The pentacene deposition was performed by thermal sublimation in a ultrahigh vacuum with a base pressure of 5×10^{-8} mbar at a rate of 7.5 \AA min^{-1} on the substrate held at room temperature. The pentacene film was 15 nm thick (~ 10 monolayers, ML) as previously published.^{55,57} Source, drain and gate electrodes were connected to a Keithley 2612 Source Meter. The electrical response was acquired by means of a home-built test-pattern holder. This system offers a compact layout and an easy-to-use monitoring of the electrical performance of our EGOFETs. The electrical measurements were carried out in lab atmosphere. The I - V transfer characteristics were performed by sweeping the gate-source voltage (V_{GS}) from +0.5 V to -0.5 V while leaving the drain-source voltage (V_{DS}) constant at -0.1 V (linear regime) for the reference device. The I - V output characteristics were carried out by sweeping V_{DS} from 0 V to -0.5 V and V_{GS} from 0 V to -0.5 V with a step of 0.1 V. The electrical measurements after DA adsorption were carried out by sweeping V_{GS} from +0.2 V to -0.4 V with $V_{DS} = -0.1$ V. The V_{GS} scan rate is around 20 mV s^{-1} and 80 mV s^{-1} for transfer and output characteristics respectively. The electrical release of DA and L-DOPA through an EGOFET has been carried out scanning the V_{GS} from 0 V to 1.1 V. Source and drain electrodes have been short-circuited and grounded, therefore the device has been operated as a two-electrode system.

Conclusions

This work was focused on the chemical adsorption of A β CyD vesicles onto Au by exploiting the well-known affinity between amino groups and this metal. The vesicle adsorption turns an inert Au surface into a multi-functional one. As a result, the coated Au is sensitive to the pH due to the presence of amine groups. Furthermore, the A β CyD-based coating can yield a partial or total screening of the Au electrode towards electroactive species bearing negative (*viz.* ferricyanide) and positive charges (*viz.* dopamine), respectively. Adsorbed A β CyD vesicles mediate both trapping and release of DA and L-DOPA by using their intrinsic host-guest properties. The proper control of the electrical bias allows a gradual drug release not only in a

standard electrochemical equipment, but also in an electronic device used as an electronic drug dispenser. Such results open the way towards bio-electronic applications, because the next generation of hi-tech platforms must be multi-functional in order to manage high-challenging tasks. Among the different functionalities, the release of drugs or chemicals is one of the most demanded.

Acknowledgements

This work was supported by the EU-project I-ONE NMP4-SL-2012-280772, and EuroBioSAS-OP-009 (ICS project).

Notes and references

- 1 K. Ariga, Q. Ji, J. P. Hill, Y. Bando and M. Aono, Forming Nanomaterials as Layered Functional Structures toward Materials Nanoarchitectonics, *NPG Asia Mater.*, 2012, **4**, 1–11.
- 2 K. Ariga, Y. Yamauchi, G. Rydzek, Q. Ji, Y. Yonamine, K. C.-W. Wu and J. P. Hill, Layer-by-Layer Nanoarchitectonics: Invention, Innovation and Evolution, *Chem. Lett.*, 2014, **43**, 36–68.
- 3 J. Szejtli, Introduction and General Review of Cyclodextrin Chemistry, *Chem. Rev.*, 1998, **98**, 1743–1753.
- 4 E. Bilensoy and A. A. Hincal, Recent Advances and Future Directions in Amphiphilic Cyclodextrin Nanoparticles, *Expert Opin. Drug Delivery*, 2009, **6**, 1161–1173.
- 5 B. J. Ravoo and R. Darcy, Cyclodextrin Bilayer Vesicles, *Angew. Chem., Int. Ed.*, 2000, **39**, 4324–4326.
- 6 A. Mazzaglia, A. Valerio, N. Micali, V. Villari, M. Giuffrè, F. Quaglia, A. Castriciano, L. Monsù Scolaro, G. Siracusano and M. T. Sciortino, Effective Cell Uptake of Nanoassemblies of a Fluorescent Amphiphilic Cyclodextrin and an Anionic Porphyrin, *Chem. Commun.*, 2011, 9140–9142.
- 7 A. McMahon, M. J. O'Neill, E. Gomez, R. Donohue, D. Forde, R. Darcy and C. M. O'Driscoll, Targeted Gene Delivery to Hepatocytes with Galactosylated Amphiphilic Cyclodextrins, *J. Pharm. Pharmacol.*, 2012, **64**, 1063–1073.
- 8 A. Scala, M. Cordaro, A. Mazzaglia, F. Risitano, A. Venuti, M. T. Sciortino and G. Grassi, Synthesis and Anti HSV-1 Evaluation of Novel Indole-3,4-diones, *MedChemComm*, 2011, **2**, 172.
- 9 F. Quaglia, L. Ostacolo, A. Mazzaglia, V. Villari, D. Zaccaria and M. T. Sciortino, The Intracellular effects of Non-Ionic Amphiphilic Cyclodextrin Nanoparticles in the Delivery of Anticancer Drugs, *Biomaterials*, 2009, **30**, 374–3782.
- 10 C. Conte, A. Scala, G. Siracusano, N. Leone, S. Patanè, F. Ungaro, A. Miro, M. T. Sciortino, F. Quaglia and A. Mazzaglia, Nanoassembly of an Amphiphilic Cyclodextrin and Zn(II)-phthalocyanine with the Potential for Photodynamic Therapy of Cancer, *RSC Adv.*, 2014, **4**, 43903–43911.

- 11 A. Mazzaglia, M. L. Bondi, A. Scala, F. Zito, G. Barbieri, F. Crea, G. Vianelli, P. Mineo, T. Fiore, C. Pellerito, L. Pellerito and M. A. Costa, Supramolecular Assemblies Based on Complexes of Nonionic Amphiphilic Cyclodextrins and a Meso-Tetra(4-sulfonatophenyl)porphyrine Tributyltin(IV) Derivative: Potential Nanotherapeutics against Melanoma, *Biomacromolecules*, 2013, **14**, 3820–3829.
- 12 N. Kandoth, E. Vittorino, M. T. Sciortino, T. Parisi, I. Colao, A. Mazzaglia and S. Sortino, A Cyclodextrin-Based Nanoassembly with Bimodal Photodynamic Action, *Chem. Eur. J.*, 2012, **18**, 1684–1690.
- 13 V. Villari, A. Mazzaglia, R. Darcy, C. M. O'Driscoll and N. Micali, Nanostructures of Cationic Amphiphilic Cyclodextrin Complexes with DNA, *Biomacromolecules*, 2013, **14**, 811–817.
- 14 M. Trapani, A. Romeo, T. Parisi, M. T. Sciortino, S. Patanè, V. Villari and A. Mazzaglia, Supramolecular Hybrid Assemblies Based on Gold Nanoparticles, Amphiphilic Cyclodextrin and Porphyrins with Combined Phototherapeutic Action, *RSC Adv.*, 2013, **3**, 5607–5614.
- 15 A. Mazzaglia, L. Monsù Scolaro, A. Mezzi, S. Kaciulis, T. De Caro, G. M. Ingo and G. Padeletti, Supramolecular Colloidal Systems of Gold Nanoparticles/Amphiphilic Cyclodextrin: a FEM-SEM and XPS Investigation of Nanostructures Assembled onto Solid Surface, *J. Phys. Chem. C*, 2009, **113**, 12772–12777.
- 16 L. Valli, G. Giancane, A. Mazzaglia, L. Monsù Scolaro, S. Conoci and S. Sortino, Photoresponsive Multilayer Films by Assembling Cationic Amphiphilic Cyclodextrins and Anionic Porphyrins at the Air/Water Interface, *J. Mater. Chem.*, 2007, **17**, 1660–1663.
- 17 L. Kergoat, L. Herlogsson, D. Braga, B. Piro, M.-C. Pham, X. Crispin, M. Berggren and G. Horowitz, A Water-Gated Organic Field-Effect Transistor, *Adv. Mater.*, 2010, **22**, 2565–2569.
- 18 L. Kergoat, B. Piro, M. Berggren, G. Horowitz and M.-C. Pham, Advances in Organic Transistor-Based Biosensors: from Organic Electrochemical Transistors to Electrolyte-Gated Organic Field-Effect Transistors, *Anal. Bioanal. Chem.*, 2012, **402**, 1813–1826.
- 19 A. Campana, T. Cramer, D. T. Simon, M. Berggren and F. Biscarini, Electrocadiographic Recording with Conformable Organic Electrochemical Transistor Fabricated on Resorbable Scaffold, *Adv. Mater.*, 2014, **26**, 3874–3878.
- 20 D. Khodagholi, T. Doublet, P. Quilichini, M. Gurfinkel, P. Leleux, A. Ghestem, E. Ismailova, T. Hervé, S. Sanaur, C. Bernard and G. G. Malliaras, In Vivo Recordings of Brain Activity using Organic Transistors, *Nat. Commun.*, 2013, **4**, 1575.
- 21 D.-H. Kim, N. Lu, R. Ghaffari, Y.-S. Kim, S. P. Lee, L. Xu, J. Wu, R.-H. Kim, J. Song, Z. Liu, J. Viventi, B. de Graff, B. Elolampi, M. Mansour, M. J. Slepian, S. Hwang, J. D. Moss, S.-M. Won, Y. Huang, B. Litt and J. A. Rogers, Materials for Multifunctional Balloon with Capabilities in Cardiac Electrophysiological Mapping and Ablation Therapy, *Nat. Mater.*, 2011, **10**, 316–323.
- 22 J. Viventi, D.-H. Kim, J. D. Moss, Y.-S. Kim, J. a. Blanco, N. Annetta, A. Hicks, J. Xiao, Y. Huang, D. J. Callans, J. a. Rogers and B. Litt, A Conformal, Bio-Interfaced Class of Silicon Electronics for Mapping Cardiac Electrophysiology, *Sci. Transl. Med.*, 2010, **2**, 24ra22.
- 23 J. Viventi, D.-H. Kim, L. Vigeland, E. S. Frechette, J. a. Blanco, Y.-S. Kim, A. E. Avrin, V. R. Tiruvadi, S.-W. Hwang, A. C. Vanleer, D. F. Wulsin, K. Davis, C. E. Gelber, L. Palmer, J. Van der Spiegel, J. Wu, J. Xiao, Y. Huang, D. Contreras, J. A. Rogers and B. Litt, Flexible, Foldable, Actively Multiplexed, High-Density Electrode Array for Mapping Brain Activity In-Vivo, *Nat. Neurosci.*, 2011, **14**, 1599–1605.
- 24 D. Son, J. Lee, S. Qiao, R. Ghaffari, J. Kim, J. E. Lee, C. Song, S. J. Kim, D. J. Lee, S. W. Jun, S. Yang, M. Park, J. Shin, K. Do, M. Lee, K. Kang, C. S. Hwang, N. Lu, T. Hyeon and D.-H. Kim, Multifunctional Wearable Devices for Diagnosis and Therapy of Movement Disorders, *Nat. Nanotechnol.*, 2014, **9**, 397–404.
- 25 I. R. Mineev, P. Musienko, A. Hirsch, Q. Barraud, N. Wenger, E. M. Moraud, J. Gandar, M. Capogrosso, T. Milekovic, L. Asboth, R. F. Torres, N. Vachicouras, Q. Liu, N. Pavlova, S. Duis, A. Larmagnac, J. Vörös, S. Micera, Z. Suo, G. Courtine and S. Lacour, Electronic Dura Mater for Long-Term Multimodal Neural Interfaces, *Science*, 2015, **347**, 159–163.
- 26 A. Ferancová and J. Labuda, Cyclodextrins as electrode modifiers, *Fresenius' J. Anal. Chem.*, 2001, **370**, 1–10.
- 27 A. Cristiano, C. W. Lim, D. I. Rozkiewicz, D. N. Reinhoudt and B. J. Ravoo, Solid-supported monolayers and bilayers of amphiphilic β -cyclodextrins, *Langmuir*, 2007, **23**, 8944–8949.
- 28 J. P. Silvestre, S. Pouline, A. V. Kabashin, E. Sacher, M. Meunier and J. H. T. Luong, Surface Chemistry of Gold Nanoparticles Produced by Laser Ablation in Aqueous Media, *J. Phys. Chem. B*, 2004, **108**, 16864–16869.
- 29 I. Reviakine and A. Brisson, Formation of supported phospholipid bilayer from unilamellar vesicles investigated by atomic force microscopy, *Langmuir*, 2000, **16**, 1806–1815.
- 30 A. Sackmann, Supported membrane: Scientific and practical applications, *Science*, 1996, **271**, 43–48.
- 31 J. Krim and G. Palasantzas, Experimental Observations of Self-Affine Scaling and Kinetic Roughening at Sub-Micron Lengthscales, *Int. J. Mod. Phys. B*, 1995, **09**, 599–632.
- 32 C. Albonetti, S. Casalini, F. Borgatti, L. Floreano and F. Biscarini, Morphological and Mechanical Properties of Alkanethiol Self-Assembled Monolayers Investigated Atomic Force Microscopy, *Chem. Commun.*, 2011, **47**, 8823–8825.
- 33 R. Donohue, A. Mazzaglia, B. J. Ravoo and R. Darcy, Cationic β -Cyclodextrin Bilayer Vesicles, *Chem. Commun.*, 2002, **7**, 2864–2865.
- 34 A. J. Bard and L. R. Faulkner, *Electrochemical Methods Fundamentals and Applications*, 2001.
- 35 S.-M. Park and J.-S. Yoo, Electrochemical Impedance Spectroscopy for Better Electrochemical Measurements, *Anal. Chem.*, 2003, **75**, 455–461.

- 36 L. W. Mark and D. A. Smith, Complex Chemical Force Titration Behavior of Amine-Terminated Self-Assembled Monolayers, *Langmuir*, 2001, **17**, 1126–1131.
- 37 G. Dryhurst, M. K. Kadish, F. Scheller and R. Renneberg, *Biological Electrochemistry*, Academic Press, vol. 1, 1982.
- 38 A. E. Sanchez-Rivera, S. Corona-Avedaño, G. Alarcón-Ángeles, A. Rojas-Hernández, M. T. Ramírez-Silva and M. A. Romero-Romo, Spectrophotometric Study on the Stability of Dopamine and the Determination of its Acidity Constants, *Spectrochim. Acta, Part A*, 2003, **59**, 3193–3203.
- 39 A. Abbaspour and A. Noori, A Cyclodextrin Host-Guest Recognition Approach to an Electrochemical Sensor for Simultaneous Quantification of Serotonin and Dopamine, *Biosens. Bioelectron.*, 2011, **26**, 4674–4680.
- 40 M. Palomar-Pardavé, S. Corona-Avedaño, M. Romero-Romo, G. Alarcón-Ángeles, a. Merkoçi and M. T. Ramírez-Silva, Supramolecular Interaction of Dopamine with β -Cyclodextrin: An Experimental and Theoretical Electrochemical Study, *J. Electroanal. Chem.*, 2014, **717–718**, 103–109.
- 41 S. Shityakov, J. Broscheit and C. Förster, α -Cyclodextrin Dimer Complexes of Dopamine and Levodopa Derivatives to Assess Drug Delivery to the Central Nervous System: ADME and Molecular Docking Studies, *Int. J. Nanomed.*, 2012, **7**, 3211–3219.
- 42 L. Tan, K.-G. Zhou, Y.-H. Zhang, H.-X. Wang, X.-D. Wang, Y.-F. Guo and H.-L. Zhang, Nanomolar Detection of Dopamine in the Presence of Ascorbic Acid at β -Cyclodextrin/Graphene Nanocomposite Platform, *Electrochem. Commun.*, 2010, **12**, 557–560.
- 43 J.-H. Yang, H. T. Kim and H. Kim, A Cyclodextrin-Based Approach for Selective Detection of Catecholamine Hormone Mixtures, *Micro Nano Syst. Lett.*, 2014, **2**, 1–10.
- 44 M. K. Zachek, A. Hermans, R. M. Wightman and G. S. McCarty, Electrochemical Dopamine Detection: Comparing Gold and Carbon Fiber Microelectrodes Using Background Subtracted Fast Scan Cyclic Voltammetry, *J. Electroanal. Chem.*, 2008, **614**, 113–120.
- 45 J. O. Zerbino and M. G. Sustersic, Ellipsometric and Electrochemical Study of Dopamine Adsorbed on Gold Electrodes, *Langmuir*, 2000, **16**, 7477–7481.
- 46 L. Kergoat, B. Piro, M. Berggren, M.-C. Pham, A. Yassar and G. Horowitz, DNA Detection with Water-Gated Organic Field-Effect Transistor, *Org. Electron.*, 2012, **13**, 1–6.
- 47 F. Buth, A. Donner, M. Sachsenhauser, M. Stutzmann and J. A. Garrido, Biofunctional Electrolyte-Gated Organic Field-Effect Transistors, *Adv. Mater.*, 2012, **24**, 4511–4517.
- 48 M. Magliulo, A. Mallardi, M. Y. Mulla, S. Cotrone, B. R. Pistillo, P. Favia, I. Vikholm-Lundin, G. Palazzo and L. Torsi, Electrolyte-Gated Organic Field-Effect Transistor Sensors Based on Supported Biotinylated Phospholipid Bilayer, *Adv. Mater.*, 2013, **25**, 2090–2094.
- 49 S. Casalini, F. Leonardi, T. Cramer and F. Biscarini, Organic Field-Effect Transistor for Label-Free Dopamine Sensing, *Org. Electron.*, 2013, **14**, 156–163.
- 50 S. Casalini, A. C. Dumitru, F. Leonardi, C. A. Bortolotti, E. T. Herruzo, A. Campana, R. F. De Oliveira, T. Cramer, R. Garcia and F. Biscarini, Multiscale Sensing of Antibody-Antigen Interactions by Organic Transistors and Single-Molecule Force Spectroscopy M., *ACS Nano*, 2015, **9**, 5051–5062.
- 51 L. Kergoat, L. Herlogsson, D. Braga, B. Piro, M.-C. Pham, X. Crispin, M. Berggren and G. Horowitz, *Adv. Mater.*, 2010, **22**, 2565–2569.
- 52 T. Cramer, A. Kyndiah, M. Murgia, F. Leonardi, S. Casalini and F. Biscarini, Double Layer Capacitance Measured by Organic Field-Effect Transistor Operated in Water, *Appl. Phys. Lett.*, 2012, **100**, 143302.
- 53 J. Guo, N. Koch, J. Schwartz and S.L. Bernaseck, Direct measurement of surface complex surface loading and surface dipole and their effect behavior, *J. Phys. Chem. B*, 2005, **109**, 3966–3970.
- 54 F. Leonardi, S. Casalini, C. Albonetti, A. Kovtun, A. Liscio and F. Biscarini, Charge-injection organic gauges to detect dopamine down to the nanomolar scale, *IEEE Trans. Electron Devices*, 2015, DOI: 10.1109/TED.2015.2491650.
- 55 S. Casalini, A. Shehu, S. Destri, W. Porzio, M. C. Pasini, F. Vignali, F. Borgatti, C. Albonetti, F. Leonardi and F. Biscarini, Organic Field-Effect Transistors as New Paradigm for Large-Area Molecular Junctions, *Org. Electron.*, 2012, **13**, 789–795.
- 56 I. D. Baikie, S. Mackenzie, P. J. Z. Estrup and J. A. Meyer, Noise and Kelvin Method, *Rev. Sci. Instrum.*, 1991, **62**, 1326–1333.
- 57 S. Casalini, A. Shehu, F. Leonardi, C. Albonetti, F. Borgatti and F. Biscarini, Hydrophilic Self-Assembly Monolayers for Pentacene-Based Thin-Film Transistors, *Org. Electron.*, 2013, **14**, 1891–1897.